Resolving the Individual Components of a pH-Induced Conformational Change

Christian Blouin,* J. Guy Guillemette,† and Carmichael J. A. Wallace*
*Department of Biochemistry and Molecular Biology, Dalhousie University, Nova Scotia B3H 4H7, Canada, and †Department of Chemistry, University of Waterloo, Ontario N2L 3G1, Canada

ABSTRACT This communication introduces a simple method to determine the pKs of microscopic ionizations from complex titration curves. We used this approach to study the alkaline transition (pH-dependent ligand exchange) of mitochondrial cytochrome c. The linearization of titration curves permitted resolution of two to three limiting microscopic ionizations. By combining these data with studies of the temperature dependence of ligand-exchange equilibria, we found evidence that the alkaline transition comprises two chemically distinct processes: the deprotonation of the alternative ligands and the break of the iron-methionine ligation bond. We also noted that, in the horse and untrimethylated *S. cerevisiae* iso-1 cytochromes c, the permissible deprotonation of the ϵ-amino group of Lys^{72} allows formation of an alkaline isomer at lower pH, with lesser stability, which leads to hysteresis in the titration curves. The linearization of the titration curves for different cytochromes c thus brings insight on the microscopic contributions to conformational stability.

INTRODUCTION

The monitoring by spectroscopy of pH-induced conformational change often generates an irregular titration curve. This is due to the multiplicity of microscopic components involved. The nature of these components and the detail of their interactions define the structure and the properties of a molecule. As a molecule passes from one conformation to another, some of these components become limiting to the transition. This study introduces the use of a linear regression of titration curves to identify the microscopic components of a ligand exchange in the protein cytochrome c.

The ligation of the heme iron in ferricytochrome c by the side chains of the protein is a pH-dependent property with five spectroscopically distinct states (I–V) (Theorell and Åkesson, 1941) The functional conformation is known as state III. The presence in this state of a band at 695 nm is diagnostic of a charge transfer between the ferric ion and the δ-sulfur atom of Met^{80}, the sixth ligand of heme iron (Schejter and George, 1964; Harbury et al., 1965; Eaton and Hochstrasser, 1967). During the transition from state III to IV, the 695-nm band disappears with an apparent pK value ranging from 8.5 to 9.5, depending on the species of origin (9.35 in the horse variant) (Moore and Pettigrew, 1990) and titration conditions (Pearce et al., 1989). The replacement of Met^{80} by another iron ligand is commonly referred to as the alkaline transition of cytochrome c.

The iron in state IV remains low spin due to coordination by strong field ligands. In yeast cytochrome c (isoform 1), NMR spectroscopy showed that state IV consists of two possible conformations. Each has as ligand at the sixth position one of two possible deprotonated lysine ϵ-NH_2 groups (Hong and Dixon, 1989). These ligands were identified in the yeast cytochrome c (iso-1) as lysines 73 and 79 (Ferrer et al., 1993; Rosell et al., 1998; Döpner et al., 1998). In the yeast variant, the apparent pK of the alkaline transition ($pK' = 8.7$) is an intermediate value between the pKs of two ionizations ($pK = 8.44$ and 8.82) (Rosell et al., 1998). In the bacterially expressed yeast cytochrome c iso-1, the apparent pK of the alkaline transition is decreased by 0.6 pK units, to ~8.1 (Pollock et al., 1998). This is hypothesized to be due to the absence of post-translational trimethylation at position 72 that makes this lysine side chain a plausible ligand once deprotonated. Animal cells do not undertake this trimethylation modification (Moore and Pettigrew, 1990). For that reason, the alternative ligands for these variants were proposed to be Lys^{72} and Lys^{79} (Pollock et al., 1998). Further observations showed that no major conformational rearrangement occurs in the protein other than the iron ligand replacement (Rosell et al., 1998).

We show in this communication that the study of limiting microscopic components reveals that, in cytochrome c, the mere absence of trimethylation at Lys^{72} in the yeast cytochrome c alters the process of its alkaline transition by generating a conformer at a lower pH. Moreover, this conformer must, to account for the hysteresis observed in the titration, overcome a high-energy barrier to equilibrate with the other, more stable, alkaline conformers. We also show that the loss of Met^{80} iron ligation is not solely determined by the ionization of the lysine ligands but is likely to involve another microscopic trigger. We finally argue that the resolution of individual protonation equilibria obtained using this analysis provides valuable information about the microscopic components that cooperate in complex phenomena such as conformational stability.

Received for publication 17 January 2001 and in final form 5 June 2001.
Address reprint requests to Dr. Carmichael J. A. Wallace, Dalhousie University, Department of Biochemistry, Nova Scotia NS, Canada B3H 4H7. Tel.: 902-494-1118; E-mail: carmichael.wallace@dal.ca.

0006-3495/01/10/2331/08 $2.00

MATERIALS AND METHODS

Mutant preparation

Site-directed mutagenesis was performed using a procedure based on the QuickChange method by Stratagene (La Jolla, Ca). The entire gene for the mutant R13K/R38K/M64L/C102T yeast iso-1-cytochrome c, and parts of the upstream and downstream untranslated regions were cut from pING4 (Inglis et al., 1991) using *Hind*III and subcloned into Bluescript KS^+ vector.

The resulting plasmid named pEW8.1 was used as the template for performing mutagenesis reactions to avoid problems originally encountered with the large 10.5-kbp pING4 phagemid when using this mutagenesis technique. For each mutagenic reaction, a set of complementary forward and reverse nucleotide primers carrying the desired mutation were synthesized at the MOBIX facility, McMaster University, Canada. The complementary oligonucleotides K72RF 5′-TACTTGACTAACCCGCG-GAAATATATTCCTGGT-3′ and K72RR 5′-ACCAGGAATATATTTC-CGCGGGTTAGTCAAGTA-3′ were the respective forward and reverse oligonucleotides used to introduce the K72R mutation as well as a *Sac*II restriction site. The complementary oligonucleotides K79RF 5′-TATATTCCTGGTACGCGTATGGCCTTTGGTGGG-3′ and K79RR 5′-CCCACCAAAGGCCATACGCGTACCAGGAATATA-3′ were used to introduce the K79R mutation as well as a *Mlu*I restriction site. The *Sac*II and *Mlu*I restriction sites were introduced by silent mutations and used for screening purposes. For each mutagenesis reaction, 50 ng of plasmid pEW8.1 DNA, 50 pmol of each of the appropriate forward and reverse primers, 5 ml of the 10X PWO buffer (Boehringer Mannheim, Laval, Canada) and 2.5 mM of each dNTP were mixed together on ice and brought to a final volume of 50 ml. The samples were heated to 85°C in an Amplitron II thermocycler (Thermolyne) before the addition of 2 units of PWO polymerase (Boehringer Mannheim) per reaction. The polymerase chain reaction parameters used consisted of 16 cycles of sequential incubations of 30 s at 95°C, 30 s at 55°C, and 10 min at 68°C. Upon completion of the amplification reaction, the samples were cooled to 37°C and 10 units of *Dpn*I endonuclease (Boehringer Mannheim) added and the samples incubated for 2 h to selectively digest the methylated parental DNA template. The nuclease-treated DNA was then used to transform XL1-Blue1 cells and the resulting colonies screened for the *Sac*II or *Mlu*I restriction site in K72R and K79R samples, respectively. We usually find a greater than 80% rate of mutagenesis using this procedure. The mutant DNA was then fully sequenced to verify the incorporation of the desired modification and rule out the production of spontaneous mutations during amplification. The mutant cytochrome c genes were cut using *Sma*I/*Hind*III from the respective plasmids and subcloned back into pING4 restricted with the same enzymes. The plasmids carrying the mutant cytochrome c genes were used to transform yeast GM3C-2 cells for expression of the protein as previously described (Inglis et al., 1991).

Reductive alkylation of lysines

Alkylation was undertaken as previously described (Wallace and Corthésy, 1987), using acetone to produce a fully alkylated isopropyl-lysine derivative. The protein was considered fully alkylated when additional reaction cycles no longer affected its chromatographic properties.

Titration of the 695-nm band

Horse cytochrome c (Boehringer Mannheim) was fully oxidized using excess potassium ferricyanide and then desalted on a Sephadex G-25 PD-10 column (Pharmacia, Canada) and brought to a final concentration of ~2.5–8 mg/ml in 50 mM potassium phosphate. The charge transfer band at 695 nm was evaluated by subtracting the absorbance at 710 nm (baseline) from that at 695 nm measured using a HP 8452A diode array spectrophotometer (Hewlett-Packard, Mississauga, Canada) for pH values typically ranging from 6.5 to 10.5 and at ~0.15-pH-unit intervals.

Data processing

Before treatment of the data using the linear regression, a nonlinear best fit of the titration curve was made to evaluate the apparent pK (pK′) of the titration and the offset in absorbance of the titration curve. This offset has to be deducted from the 695-nm peak height to fit to Eq. 2. Equation 1, with A_{695nm}, the absorbance of the 695-nm band; A_{max}, the maximal band height at neutral pH; K_a, the ionization constant, and $[H^+]$, the concentration of protons, is based on the mathematical definition of an ionization. By rearranging Eq. 1, we obtain a linear form as shown in Eq. 2.

$$A_{695\ nm} = \frac{A_{max}}{1 + (K_a/[H^+])} \quad (1)$$

$$\frac{A_{695\ nm}}{[H^+]} = \frac{A_{max}}{K_a} - \frac{A_{695\ nm}}{K_a} \quad (2)$$

By plotting $A_{695\ nm}/[H^+]$ versus $A_{695\ nm}$, an ionization constant can be calculated from the slope of the linear function. Most samples assayed yielded a function made up of two or three linear segments. A corresponding ionization constant could be then calculated for each of these segments. The precision of measurements of pK was typically within ±0.05 unit of pH.

Titration at equilibrium

An aliquot of a master solution of commercial horse cytochrome c (50 mM Na^+ phosphate, pH 7.0) was treated with potassium ferricyanide to oxidize the protein and buffer exchanged into 50 mM sodium phosphate pH 9.2 or 10.5 using a G-25 resin in a PD-10 desalting column. From there, the titration was either immediately performed in ~0.1-pH-unit increments to pH 7.4 or to pH 10.5 or after incubation at room temperature for 10 min. Finally, the titration curve was sampled over a few data points in the pH range of 10.5–11 to determine the value of the baseline of absorbance in the absence of a 695-nm band. The corresponding fragments of the titration curves were then mathematically processed as described.

Determination of thermodynamic parameters

Determination of thermodynamic parameters was performed using the graphical method of Van't Hoff. Maximal absorbance was evaluated at pH 6.5. Then the samples were titrated to a pH 8.70 ± 0.02, corresponding to the apparent transition midpoint in yeast cytochrome c and left to equilibrate in a thermostated cuvette holder HP 89090A (Hewlett-Packard). The 695-nm peak height was monitored over 20–34°C using increments of 2°C. A final measurement was made at pH ≈ 10.5 to assess the baseline of absorbance at 695 nm.

RESULTS

Linearization of a pseudosigmoid titration curve

The alkaline transition was monitored at high cytochrome c concentration to increase the clarity of the measurement of this faint signal. The irregularities of the pseudosigmoidal titration curve of the 695-nm band of ferricytochrome c revealed two or three linear segments, forming a broken line when the spectroscopic signal over the concentration of

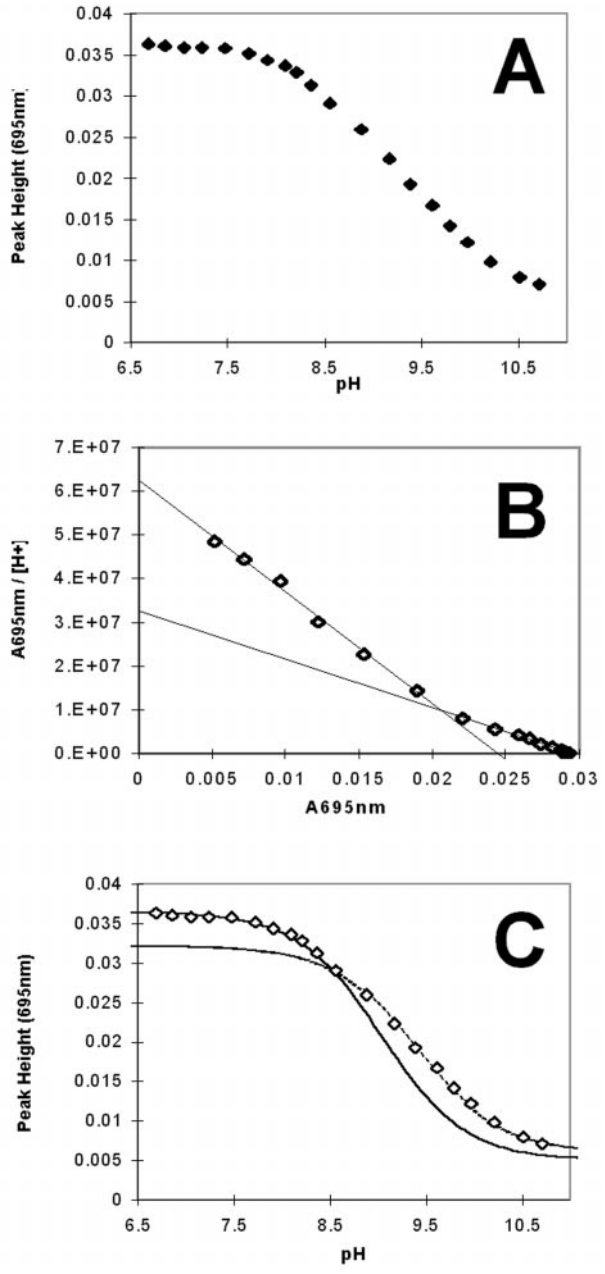

FIGURE 1 Deconvolution of the transition IV→III in horse heart cytochrome c. (*A*) The 695-nm peak height titration; (*B*) Linear regression of the transition and least-squares best fit of its two linear segments; (*C*) Titration curve reconstituted from K_a measured in *B* superimposed with data shown in *A*.

protons was plotted against the signal itself (as per Eq. 2 in Materials and Methods). The linearized plots show a sharp change in slope over the course of the titration. From such a biphasic plot, it is possible to reconstitute a series of overlapping sigmoidal components from the discrete pK values and pH window to which they are limited. Fig. 1 displays the processing of the data for the state IV to III transition in the horse protein as an example. Parameters calculated from the plot reproduce with accuracy the irregular shape of the titration curve. From such linearity, it is clear that the non-ideal character of the titration curve is not originating from the sum of multiple microscopic titration curves.

$$\frac{d[A/[H^+]]}{dA} = -\frac{1}{K_a} \tag{3}$$

Equation 3 shows the derivative of the described linear plot, where A represents the absorbance at 695 nm, [H+] the concentration of protons in solution, and K_a, the ionization constant of a single ionizing group.

$$A = \frac{A_{max1}}{1 + \left(\frac{K_1}{[H^+]}\right)} + \frac{A_{max2}}{1 + \left(\frac{K_2}{[H^+]}\right)} \tag{4}$$

$$\frac{d[A/[H^+]]}{dA} = -\left(\frac{[H^+] + K_2}{[H^+] + K_1K_2}\right) \tag{5}$$

In the case where the signal of two ionizations would be additive, the observed titration curve would be determined by Eq. 4, where K_1 and K_2 are the ionization constants of two of these ionizing groups. If the titration curve of two additive signals were plotted according to Eq. 2, no linear segments would be observed because the derivative as shown in Eq. 5 depends on the concentration of protons and hence is pH dependent.

Asymmetry of the alkaline transition in horse cytochrome c

The alkaline transition of the horse mitochondrial cytochrome c does not follow an identical path in both directions as shown in Fig. 2. Direct observation of this hysteresis is almost impossible, but the sensitivity provided by the linearization of the data makes the phenomenon evident.

The hysteresis is assumed to arise from a difference in mechanism of the transition that depends on the direction of the titration. The linear regression treatment was used to determine which of these mechanisms the protein would adopt when protein was allowed to equilibrate at mid-transition.

Table 1 shows the observed pK under different titration conditions. The forward mechanism (state III to IV) has two limiting ionizations with $pK_{F1} = 8.9 \pm 0.1$ and $pK_{F2} = 9.25 \pm 0.02$. The reverse mechanism also reveals two limiting ionizations with $pK_{R1} = 9.08 \pm 0.03$ and $pK_{R2} = 9.38 \pm 0.05$. According to Table 1, if the protein is left to equilibrate at the midpoint of the transition, the reverse pathway is observed regardless of the direction of the titration.

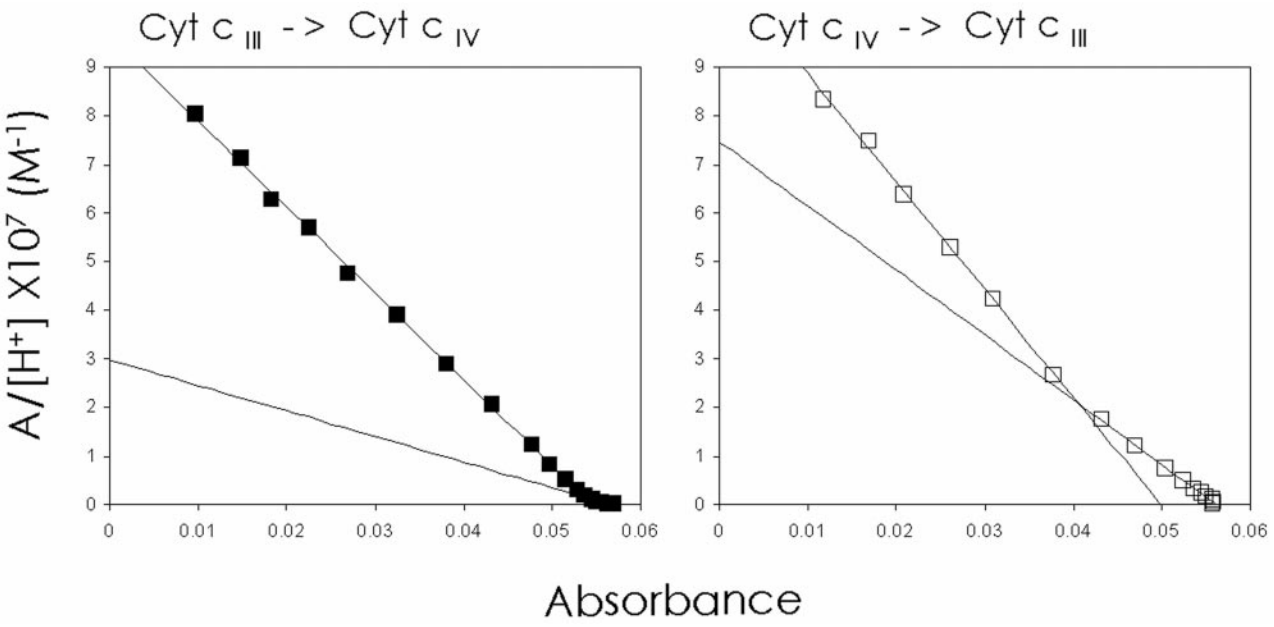

FIGURE 2 Hysteresis in the alkaline transition of horse cytochrome c. Linearized titration plot of the 695-nm band from functional state III to IV (■) and state IV to III (□).

Alkylamine derivative of mitochondrial horse cytochrome c

A total lysine alkylation was performed and the effective pKs of the alkaline transition were evaluated in an attempt to determine whether the visible ionizations were due to ionization of lysine ϵ-NH_2 groups. Alkylation of amino groups to secondary amines will alter their pK without changing their ability to donate or accept a hydrogen bond as well as coordinate the heme iron. In the isopropyl-lysine secondary amine, we observe that the limiting ionizations are shifted by $\sim+0.6$ unit of pH with pKs of 9.65 ± 0.01, 10.02 ± 0.05, and 10.43 ± 0.07. It is noteworthy that the alkaline transition of this cytochrome c derivative has three limiting effective pKs and shows no hysteresis.

TABLE 1 Profile of effective pKs of horse cytochrome *c* alkaline transition following rapid pH change by buffer exchange

Titration	Initial pH	Delay (min)	Limiting ionization			
			pK_{F1}	pK_{R1}	pK_{F2}	pK_{R2}
Forward*	7.0	10+†	8.9 (1)		9.25 (2)	
	9.20‡	0			9.24 (4)	
	9.20	10				9.33 (4)
Reverse	10.5	0		9.08 (3)		9.38 (5)
	9.20	0	8.95 (6)	9.14 (5)		
	9.20	10	8.82 (6)	9.13 (5)		

All sample stocks were at pH 7.0 and then taken to the initial pH by buffer exchange. The numbers in parentheses indicate the precision of the last significant number.
*Titration to alkaline pH.
†No buffer exchange was performed.
‡Arbitrarily chosen pH, near the midpoint of the transition.

Alkaline transition of yeast cytochrome c

The alkaline transition of the *S. cerevisiae* iso-1 cytochrome *c* does not show any hysteresis. As shown in Fig. 3, its transition is determined by two effective pKs of 8.59 ± 0.01 and 8.9 ± 0.1. A large number of *S. cerevisiae* mutant proteins were screened for significant irregularity in the

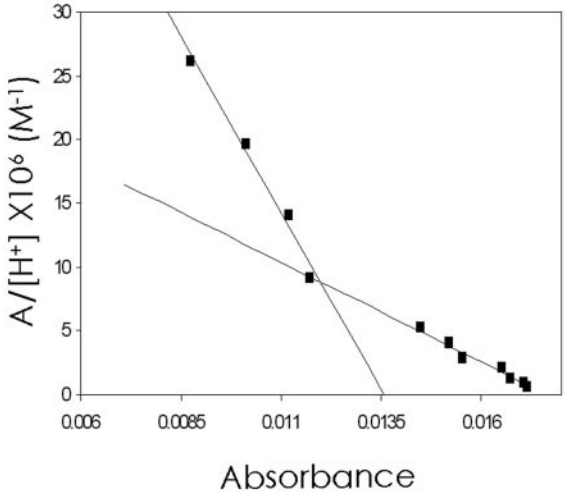

FIGURE 3 Linear regression of the alkaline transition of *S. cerevisiae* cytochrome c (iso-1 C102T).

effective pK profile of their alkaline transition. In all cases except one, which will be presented later, no hysteresis was observed. The effective pK measured in 14 of these mutants group into three ionizations with pK values of 8.01 ± 0.06, 8.53 ± 0.06, and 8.85 ± 0.09 (C. Blouin and C. J. A. Wallace, unpublished). These suggest that there are three limiting ionizations contributing to the relative distribution of state III and state IV in the yeast cytochrome c, although most mutants were limited by only two of the possible ionizations.

Position 72 and hysteresis in the yeast cytochrome c

The *Escherichia-coli*-expressed *S. cerevisiae* isoform-1 cytochrome c is identical in every way to the endogenously expressed mitochondrial cytochrome c, except for the absence of a post-translational trimethylation at position 72. However, the nature of the alkaline transition of this protein differs in a significant fashion.

First, similar to the horse protein, the alkaline transition of Tml72K shows hysteresis with regard to the direction of the titration. The two effective pKs of 8.59 ± 0.01 and 8.9 ± 0.1 in the wild type are replaced by a different set of pKs 7.8 ± 0.1 and 8.49 ± 0.06 in the forward direction and 8.0 ± 0.1, 8.35 ± 0.07, and 8.56 ± 0.05 in the reverse direction (Fig. 4).

Resolving two independent equilibria in Tml72R

The substitution of the trimethyl-lysine at position 72 by an arginine yielded some surprising results. Fig. 5 shows that the bleaching of the 695-nm charge transfer band is concomitant with the appearance of a shoulder with its center at 602 nm.

These two spectroscopic characteristics are, however, not the consequence of a single chemical process. The linearization of these two spectroscopic events yields two different sets of effective pKs; also, the thermodynamics of each equilibrium differ (Fig. 6), suggesting the presence of two distinct chemical equilibria for each spectroscopic change.

The appearance of a shoulder around 600 nm was also observed in the mutant K79R. Effective pKs for these two mutants are tabulated and presented in Table 2. Mutant K79R was targeted because of the possible implication of Lys^{79} in the alkaline transition. In this case, both spectroscopic events occur with an identical effective pK of 8.2 ± 0.02. However, the temperature dependence of its equilibrium suggests that the two spectroscopic features are diagnostic of two distinct processes.

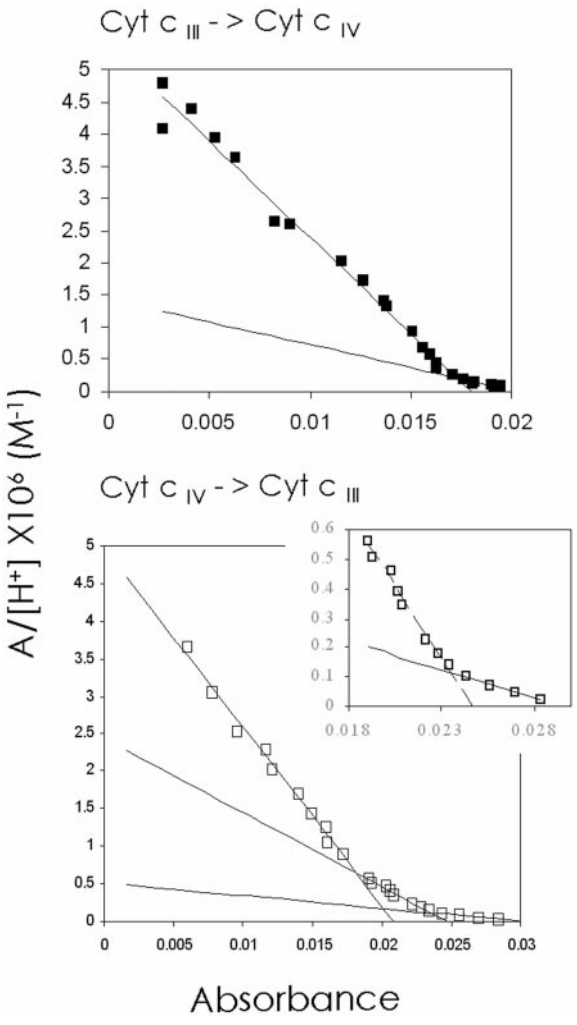

FIGURE 4 Hysteresis of the alkaline transition of *S. cerevisiae* Tml72K cytochrome c (iso-1 C102T), resolved using a linear regression relationship. Upper part of the transition from state IV to III is magnified in upper corner.

DISCUSSION

Microscopic and macroscopic ionizations

In this study, effective pKs were determined in a variety of cytochrome c mutants in an attempt to assign them to ionizing residues in the protein. The two measured pK values in *S. cerevisiae* (8.60 and 8.9) are related to the apparent pK of the alkaline transition of mutant K79A (pK_{K73} = 8.44) and K73A (pK_{K79} = 8.82) (Rosell et al., 1998). These investigators concluded that the apparent pK of the wild-type protein was an average of the microscopic pKs for these two alternative ligands. The values extracted from Fig. 3 show that these two ionizations determine the course of the alkaline transition in the wild-type cytochrome c. However, the titration curve is not a sum of these ionizations but rather an overlay of them.

We have shown that each ionizing component consecutively limits the transition over a small domain of pH. Each

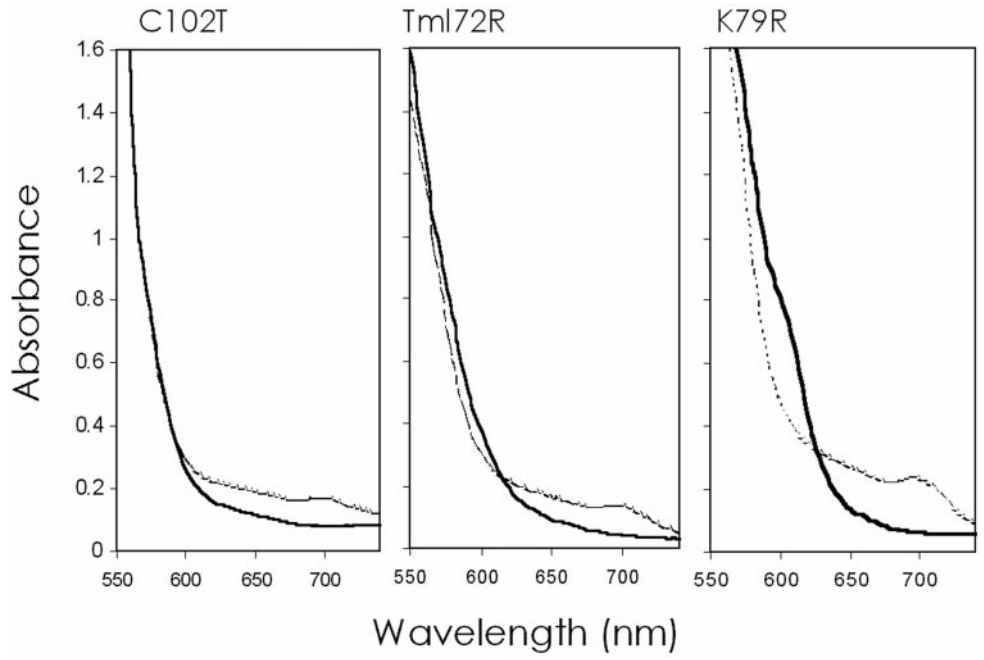

FIGURE 5 Spectra of cytochromes c in the spectroscopic states III and IV. The spectra of the various states were measured at pH 6.96 for state III (— — —) of samples and state IV (——) were measured at pH 10.11 (C102T), 10.23 (Tml72R), and 9.78 (K79R).

of them is thus stabilizing either one of the two conformations associated with either spectroscopic state in a binary fashion. The transition between the states is likely to have a cooperative nature. Although the conformations at alkaline pH are yet unknown, it was demonstrated that states IV_{73} and IV_{79} of cytochrome c are near native, stable, and ordered conformers (Rosell et al., 1998; Döpner et al., 1998). Also, thermodynamics extrapolated to a null ionic strength in fact shows that the transition is mostly enthalpic, having small positive or even slightly negative entropy (Battistuzzi et al., 1999). For this reason, we conclude that linearization of a titration curve allows resolution of coop-

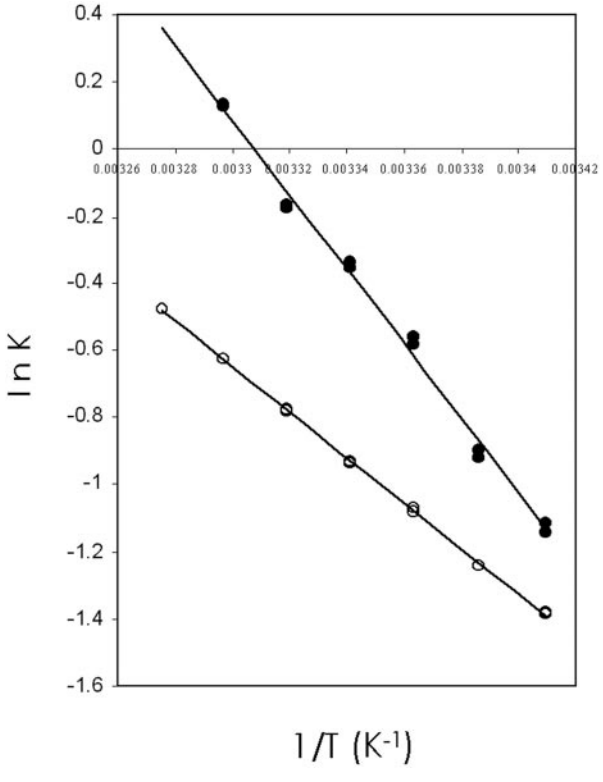

FIGURE 6 Van't Hoff plot of the spectroscopic changes observed at 695 nm (●) and 602 nm (○) at pH 8.35 in mutant Tml72R.

TABLE 2 Thermodynamic parameters calculated from Van't Hoff plots for some alkaline transition-associated equilibria

Sample	Equilibrium*	Microscopic pK(s)	ΔH (Kj/mole)
Wild type	695 nm†	8.59 ± 0.01	59.6 ± 0.8
Yeast iso-1		8.8 ± 0.1	
Wild type Horse‡	695 nm		54
Iso-1-Tm172K	695 nm		42 ± 1
Iso-1-Tml72R	695 nm	8.42 ± 0.02	76 ± 4
	602 nm§	8.59 ± 0.07	56 ± 3
		9.25 ± 0.08	
Iso-1-K79R	695 nm	8.20 ± 0.02	80.3 ± 0.8
	595 nm§	8.20 ± 0.02	93 ± 2

*Temperature dependence of the conformational equilibrium detectable by the spectroscopic band of noted wavelength relative to its maximum height.
†A sulfur-iron charge transfer band. Characteristic of state III ferricytochrome *c*.
‡As presented in Davies *et al.*, 1993.
§Characteristic of a weak-field iron ligand replacing Met 80 as sixth iron ligand.

erative microscopic ionizing components that could not be individually resolved using other methods.

Insight into the mechanism of the alkaline transition

Evidence presented in this study agrees with previously published data that the microscopic course in events of the alkaline transition is determined by the deprotonation of the alternative iron ligands. Because the only difference between the variant Tml72K and the yeast wild type is the absence of trimethylation (Pollock et al., 1998) and because Tml72K is the only yeast cytochrome c, to our knowledge, that shows hysteresis for the alkaline transition, we propose that this asymmetry in mechanism is provoked by the ionization of the ϵ-amino group of Lys^{72}. NMR evidence indicates that a spectroscopic state IV is observed at lower pH in the titration of the Tml72K variant (Pollock et al., 1998), which is also observed in this study with a pK of 7.80 ± 0.1.

We propose that the structural basis for hysteresis arises from the formation at a lower pH of a conformer of the spectroscopic state IV_{72}. Pollock and co-workers (1998) also mentioned that the conformation of this low-pH state IV is, however, not as thermodynamically stable as the other alkaline conformers. To account for a slow rate of equilibration, this conformer must then have to overcome a high-energy barrier to equilibrate with the more stable conformers IV_{73} and IV_{79}. Indeed, computed models of conformers of spectroscopic state IV indicate that the local rearrangements necessary to bring Lys^{73} or Lys^{79} to the iron coordination sphere are minimal compared with those required for Lys^{72} to ligate the heme metal ion (Blouin and Wallace, unpublished results).

Evidence of multiple equilibria in a single transition

A band at around 600 nm is acknowledged to be diagnostic of a high-spin heme iron, which is not present in wild-type state IV and therefore excludes Lys73 and 79 as alkaline ligands in these mutants. Linearization of the concomitant appearance of a shoulder in mutant Tml72R indicates that the presence of this high-spin species is not determined by the same microscopic ionization that bleached the 695-nm band. The thermodynamics of their equilibria also indicate that these two events are chemically distinct. Similarly, the formation of a high-spin species in mutant K79R is part of a different equilibrium but appears to be triggered by the same microscopic ionizing group (Table 2).

The failure to replace the Met^{80} side chain by one of the lysines in these mutants may arise from the nature of the interaction of these arginine side chains with their local environment. The failure to break the hydrogen bond between Ser^{47} and position 79 (Louie and Brayer, 1990) in the alkaline conformation of K79R, known to be critical to the stability of the heme crevice (Osheroff et al., 1980), may forbid the backbone displacement necessary for the introduction of the ϵ-amine of Lys^{73} and may instead force the introduction of a high-field ligand, such as a water molecule, into the iron coordination sphere. In both cases, if the second ligand cannot properly ligate the iron, another factor must therefore prevent Met^{80} from keeping its place as a ligand.

The identity of this weak-field ligand that provokes the high-spin species in the alkaline conformation is unknown. In Tml72R, it appears that the formation of the high-spin species coincides with ionizations found in the wild-type protein (Table 2), hypothesized to be those of lysines 73 and 79. This leaves the displacement of the δ-S of Met^{80} to be triggered by a third microscopic ionization at 8.42 ± 0.02, also visible in the transition III to IV of the unrelated variant Tml72K.

The identity of this microscopic ionization (termed the trigger by several workers) also remains open. Some candidates have been proposed in the past, including the ionization of Tyr^{67} (Davies et al., 1993; Luntz et al., 1989), a buried water molecule (Takano and Dickerson, 1981) that has been the topic of previous investigations (Lett et al., 1996; Berghuis et al., 1994). Also, an intriguing heme propionate with an apparent pK similar to the apparent pK of the alkaline transition in the horse protein (Hartshorn and Moore, 1989) is hypothesized to influence the apparent pK of the alkaline transition in tuna (Tonge et al., 1989).

In Tml72R, the difference in pK between the displacement of the Met^{80} side chain from the iron coordination sphere and the ionization of the alternative ligands suggests that the alkaline transition proceeds via an intermediate conformation that does not involve lysine ligation. An intermediate of the alkaline transition was earlier postulated by research groups who studied the phenomenon using stop-flow kinetics (Pearce et al., 1989; Davies et al., 1993) and was characterized in mutant Phe82Trp (Rosell et al., 2000). From this later work, the iron ligand in this intermediate is more likely to be Tyr^{67} or a hydroxide ion rather than a loosely bound Met^{80}.

From structural comparison of the horse and yeast proteins, one cannot explain the large difference ($\sim$0.7 units) in apparent pK of their respective alkaline transitions. However, the stability of this third ionization in both states is likely to account for the large interspecies variation. The abnormally high pK of one of the buried heme propionate appears to us likely to be sensitive to the minute interspecies variations in the stabilization of this protonated group at neutral pH.

CONCLUSION

This paper introduced a method of data treatment that allows the microscopic ionizations that limit a spectroscopic

transition to be resolved. We have shown that a complex titration curve can be deconvoluted into simple ionization events using a graphical method. Another method of deconvolution presented by Onufrief and co-workers appears to be more robust in cases of additive signals but requires a different and much more involved mathematical treatment (Onufrief et al., 2001).

In the system presented in this study, the alkaline transition of mitochondrial cytochrome c successfully resolved concomitant pH-induced conformational changes and provided insight into the mechanism by which the protonation state of a few key groups impact on structure and function of this electron transport protein.

We thank A. Brigley and J. Hankins for technical assistance, K. Black for proofreading this manuscript, Dr. S. Bearne for helpful discussion, and Dr. A. G. Mauk for his gift of the pBPCY3 plasmid.

This research was supported by NSERC of Canada (C.W.) and the Sumner doctoral fellowship (C.B.).

REFERENCES

Battistuzzi, G. M., M. Borsari, L. Loschi, A. Martinelli, and M. Sola. 1999. Thermodynamics of the alkaline transition of cytochrome c. *Biochemistry.* 38:7900–7907.

Berghuis, A. M., J. G. Guillemette, G. McLendon, F. Sherman, M. Smith, and G. D. Brayer. 1994. The role of a conserved internal water molecule and its associated hydrogen bond network in cytochrome c. *J. Mol. Biol.* 236:786–799.

Davies, A. M., J. G. Guillemette, M. Smith, C. Greenwood, A.G. P. Thurgood, A. G. Mauk, and G. R. Moore. 1993. Redesign of the interior hydrophilic region of mitochondrial cytochrome *c* by site directed mutagenesis. *Biochemistry*. 32:5431–5435

Döpner, S. P., P. Hildebrand, F. I. Rosell, A. G. Mauk. 1998. Alkaline conformational transitions of ferricytochrome c studied by resonance Raman spectroscopy. *J. Am. Chem. Soc.* 120:11246–11255

Eaton, W. A., and R. M. Hochstrasser. 1967. Electronic spectrum of single crystals of ferricytochrome-c. *J. Chem. Phys.* 46:2533–2539.

Ferrer, J. C., J. G. Guillemette, R. Bogumil, S. C. Inglis, M. Smith, and A. G. Mauk. 1993. Identification of Lys79 as an iron ligand in one form of alkaline yeast iso-1-ferricytochrome c. *J. Am. Chem. Soc.* 115: 7507–7508.

Harbury, H. A., J. R. Cronin, M. W. Fanger, T. P. Hettinger, A. J. Murphy, Y. P. Myer, and S. N. Vinogradov. 1965. Complex formation between methionine and a heme peptide from cytochrome c. *Proc. Natl. Acad. Sci. U.S.A.* 52:1658–1664.

Hartshorn, R. T., and G. R. Moore. 1989. A denaturation-induced proton-uptake study of horse ferricytochrome c. *Biochem. J.* 258:595–598.

Hong, X. L., and D. W. Dixon. 1989. NMR study of the alkaline isomerization of ferricytochrome c. *FEBS Lett.* 246:105–108.

Inglis, S. C., J. G. Guillemette, J. A. Johnson, and M. Smith. 1991. Analysis of the invariant Phe82 residue of yeast iso-1-cytochrome c by site-directed mutagenesis using a phagemid yeast shuttle vector. *Protein Eng.* 4:569–574.

Lett, C. M., A. M. Berghuis, H. E. Frey, J. R. Lepock, and J. G. Guillemette. 1996. The role of a conserved water molecule in the redox-dependent thermal stability of iso-1 cytochrome c. *J. Biol. Chem.* 271: 29088–29093.

Louie, G. V., and G. D. Brayers. 1990. High-resolution refinement of yeast iso-1-cytochrome c and comparisons with other eukaryotic cytochromes c. *J. Mol. Biol.* 214:527–555.

Luntz, T. L., A. Schejter, E. A. Garber, and E. Margoliash. 1989. Structural significance of an internal water molecule studied by site- directed mutagenesis of tyrosine-67 in rat cytochrome *c*. *Proc. Natl. Acad. Sci. U.S.A.* 86:3524–3528.

Moore, G. R., and G. W. Pettigrew. 1990. Cytochrome c: Evolutionary, Structural and Physicochemical Aspect. Springer-Verlag, New York.

Onufrief, A., D. A. Case, and G. M. Ullmann. 2001. A novel view of pH titration in biomolecules. *Biochemistry.* 40:3413–3419

Osheroff, N. D., D. Borden, W. H. Koppenol, and E. Margoliash. 1980. Electrostatic interactions in cytochrome c. The role of interactions between residues 13 and 90 and residues 79 and 47 in stabilizing the heme crevice structure. *J. Biol. Chem.* 255:1689–1697.

Pearce, L. L., A. L. Gartner, M. Smith, and A. G. Mauk. 1989. Mutation-induced perturbation of the cytochrome c alkaline transition. *Biochemistry.* 28:3152–3156. mcPollock, W. B., F. I. Rosell, M. B. Twitchett, M. E. Dumont, and A. G. Mauk. 1998. Bacterial expression of a mitochondrial cytochrome c. Trimethylation of Lys72 in yeast iso-1-cytochrome c and the alkaline conformational transition. *Biochemistry.* 37:6124–6131.

Rosell, F. I., J. C. Ferrer, and A. G. Mauk. 1998. Proton-linked protein conformational switching: definition of the alkaline conformational transition of yeast iso-1-ferricytochrome c. *J. Am. Chem. Soc*. 120: 11234–11245.

Rosell, F. I., T. R. Harris, D. P. Hildebrand, S. Dopner, P. Hildebrandt, and G. Mauk. 2000. Characterization of an alkaline transition intermediate stabilized in the Phe82Trp variant of yeast iso-1-cytochrome c. *Biochemistry*. 39:9047–9054.

Schejter, A., and P.George. 1964. The 695-mμ band of ferricytochrome c and its relationship to protein conformation. *Biochemistry.* 3:1045–1049.

Takano, T., and R. E. Disckerson. 1981. Conformation change of cytochrome *c*. I. Ferrocytochrome c structure refined at 1.5 Å resolution. *J. Mol. Biol*. 153:79–94.

Theorell, H., and Å. Åkesson. 1941. Studies on cytochrome c. *J. Am. Chem. Soc.* 63:1804–1820.

Tonge, P., G. R. Moore, and C. W. Wharton. 1989. Fourier-transform infra-red studies of the alkaline isomerization of mitochondrial cytochrome c and the ionization of carboxylic acids. *Biochem. J.* 258: 599–605.

Wallace, C. J. A., and B. E. Corthésy. 1987. Alkylamine derivatives of cytochrome c. Comparison with other lysine-modified analogues illuminates structure/function relations in the protein. *Eur. J. Biochem.* 170:293–298.

Yang, A. S., and B. Honig. 1993. On the pH dependence of protein stability. *J. Mol. Biol.* 231:458–474.